Astron. Astrophys. 336, 385–392 (1998)

ASTRONOMY AND ASTROPHYSICS

Submilliarcsecond shift of the brightness peak of the radio sources 1928+738 and 2007+777

J.C. Guirado[1], **J.M. Marcaide**[1], **E. Ros**[1], **M.I. Ratner**[2], **I.I. Shapiro**[2], **A. Quirrenbach**[3], **and A. Witzel**[4]

[1] Departamento de Astronomía, Universitat de València, E-46100 Burjassot, Valencia, Spain
[2] Harvard-Smithsonian Center for Astrophysics, Cambridge, MA 02138, USA
[3] Max Planck Institut für Extraterrestrische Physik, Postfach 1603, D-85740 Garching bei München, Germany
[4] Max Planck Institut für Radioastronomie, Postfach 2024, D-53010 Bonn, Germany

Received 6 January 1998 / Accepted 21 April 1998

Abstract. From two sets of very-long-baseline interferometry (VLBI) observations, one each at 5 GHz (1985.77) and at 2.3 and 8.4 GHz simultaneously (1988.83), of the quasar 1928+738 phase-referenced to the BL Lac object 2007+777, we infer a change in their relative position of 0.74±0.22 milliarcseconds (mas) along a position angle of –9°±25°, where the quoted standard errors account for errors in our models of the geometry of the interferometric array, the atmosphere, and the source structure. This change is interpreted as an (inadvertent) shift of the reference point selected in the structure of 1928+738, due to the presence of an emerging component; different opacity effects in the three observing frequency bands may also be a significant contributor.

Key words: astrometry – techniques: interferometric – quasars: individual: 1928+738 – quasars: individual: 2007+777

1. Introduction

Astrometric VLBI observations of extragalactic radio sources are the most effective tool to define a quasi-inertial reference frame (e.g., Johnston et al. 1995). With phase-delay astrometry, bounds on the proper motion of several radio sources have been measured (e.g., Bartel et al. 1986; Marcaide et al. 1994). In these studies, the variability of the structure of the radio sources, and the consequent difficulty in locating a fixed reference point on the radio map, dominate the astrometric error budget (up to 80% of the overall standard error of the proper-motion measurement quoted by Marcaide et al. 1994).

When proper motion is measured, there is no guarantee that the motion corresponds to that of the center of mass of the target source, since the structure of the reference source and its variability introduce uncertainty in the registration of maps from multiple epochs of observation. Registration is more reliable when the reference source has more compact structure or when the reference and target sources possess jets oriented more nearly orthogonal to each other. The latter is the case for the radio source pair 1928+738 and 2007+777. The inner parts of their superluminal jets are oriented with position angle (PA) ∼165° and 260°, respectively, and the relative motions detected in right ascension and declination can be assigned to 1928+738 with reasonable confidence.

In this paper we report a comparison of two determinations of the relative position of the radio sources 1928+738 and 2007+777, one each made at 5 GHz and at 8.4/2.3 GHz (simultaneously). The 5 GHz observations were reported by Guirado et al. 1995a (hereafter G95); therefore we focus here on the 8.4/2.3 GHz observations. We briefly describe the astrometric analysis and compare the resultant relative position with that obtained at 5 GHz.

Table 1. Observations of 1928+738 phase-referenced to 2007+777[1]

Epoch	Antennas[2]	Frequencies (GHz)
9 October 1985 (1985.77)[3]	B,L,F,K,O	5
28 October 1988 (1988.83)[4]	B,L,F,M,T	8.4 & 2.3

[1] In both experiments we used the MarkIII system in mode B (Rogers et al. 1983). The data were correlated at the MPIfR (Bonn) correlator.
[2] The symbols correspond to the following antennas (with diameter and location given in parentheses); B, Effelsberg (100 m, Germany); L, Medicina (32 m, Italy); F, Fort Davis (26 m, Texas); K, Haystack (37 m, Massachusetts); O, Owens Valley (40 m, California); M, DSS63 (70 m, Spain); T, Onsala (20 m, Sweden).
[3] See G95.
[4] The reference frequencies for the astrometric observables were 8413 and 2275 MHz for the 8.4 and 2.3 GHz frequency bands, respectively. B did not have a 2.3 GHz receiver and recorded at 8.4 GHz only.

2. Observations

On 1985 October 9-10, we made VLBI observations at 5 GHz with the array shown in Table 1. The details of these observations and the results obtained from them have already been published (G95). On 1988 October 28-29, we made a similar set of VLBI observations of the same sources, but at 8.4 and 2.3 GHz simultaneously (see Table 1).

Send offprint requests to: J.C. Guirado

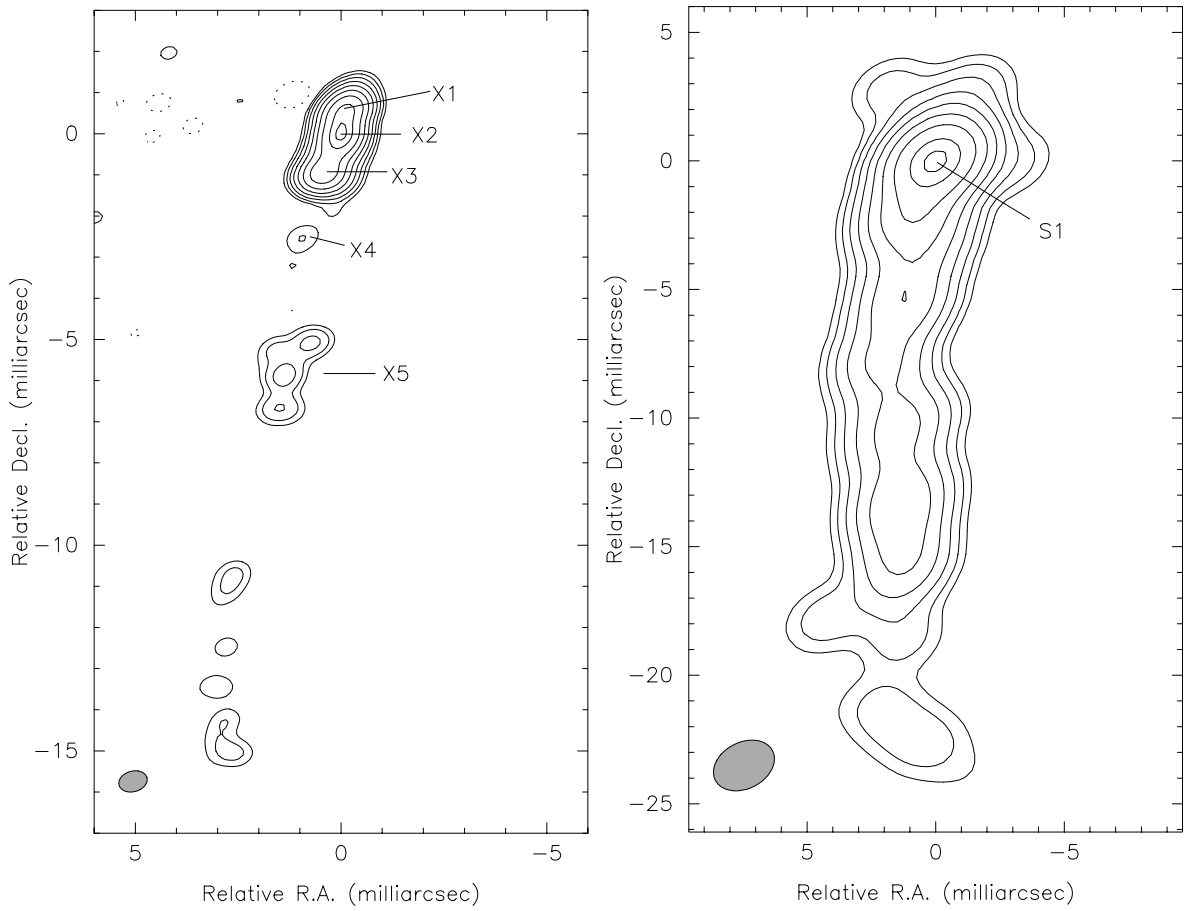

Fig. 1. Hybrid maps of 1928+738 at 8.4 (left image) and 2.3 GHz at 1988.83. Contours are -0.5,0.5,1,2,4,8,16,32,64, and 90% of the peak of brightness for each map, which is 1.1 and 0.9 Jy/beam for 8.4 and 2.3 GHz, respectively. The corresponding synthesized beam is shown at the bottom left corner of each map. The origin of each map is located at the point of maximum brightness (the two origins do not necessarily correspond to the same point on the sky). Note the difference in scale of the maps.

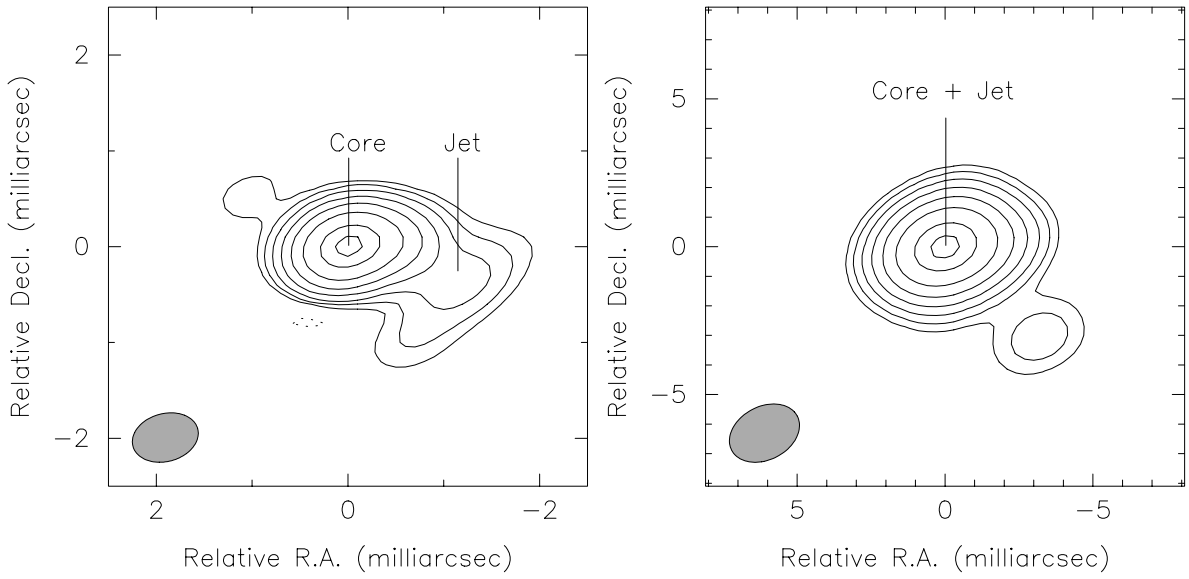

Fig. 2. Hybrid maps of 2007+777 at 8.4 (left image) and 2.3 GHz at 1988.83. Contours are -0.5,0.5,1,2,4,8,16,32,64, and 90% of the peak of brightness for each map, which is 1.7 and 0.7 Jy/beam at 8.4 and 2.3 GHz, respectively. The corresponding synthesized beam is shown at the bottom left corner of each map. The origin of each map is located at the point of maximum brightness (the two origins do not necessarily correspond to the same point on the sky). Note the difference in scale of the maps.

3. Reduction of astrometric data at 8.4 and 2.3 GHz

The data-reduction procedure for the 8.4 and 2.3 GHz observations was similar to that followed for the 5 GHz data (G95); therefore, we will describe it only briefly, emphasizing those aspects of the reduction that differed significantly.

For each source and frequency band, we corrected the phase delays for their inherent (multiple) 2π–ambiguities; to make this correction, we first constructed a model of the array geometry based on a consistent set of antenna coordinates, source coordinates, and Earth-orientation parameters from the International Earth Rotation Service (IERS) Annual Report for 1993 (IERS 1994). We calculated site coordinates at epoch 1988.83 from the 1993.00 tabulated coordinates and rates of the IERS Terrestrial Reference Frame; UT1-UTC, Earth's pole coordinates, and corrections to the model of the Earth's nutation in longitude and obliquity at the time of each observation were interpolated from the daily estimates provided by IERS. We used these parameters in an extensively improved version of the VLBI3 program (Robertson 1975) to remove most of the multiple 2π–ambiguities in the phase delays via a weighted-least-squares analysis of the phase delays and phase-delay rates; afterwards, we used interactive PGPLOT-based software to correct the (few) remaining ambiguities and to check the "phase connection" by inspection of the phase closure of each antenna triangle.

We then corrected for the remaining "overall ambiguities" (integer multiples of the radio-frequency period by which the phase delays for one source might be offset from those of the other at each station and frequency band) by estimating them in our weighted-least-squares analysis. Since, at this stage of the data reduction, some important effects, such as plasma delay, were not yet included in the model, the estimates differed by up to one third of a period from integer numbers of 2π's. Nevertheless, we made a first correction by changing these estimates to the nearest integral multiple. These values were revised after we made a plasma correction to the phase delay (see below).

3.1. Reference-point selection

To compare our results with those previously reported, we defined reference points in the images of the two radio sources. The structure and evolution of these sources have been extensively studied by Eckart et al. (1986, 1988), Witzel et al. (1988), Schalinski (1990), and Hummel et al. (1992). Our main interest here is to identify features in the sources that may serve as appropriate reference points for astrometry. For each source at each frequency, we present in Figs. 1 and 2 our hybrid maps computed with DIFMAP standard techniques (Shepherd et al. 1995). For each source and frequency band, we initially chose the reference point to correspond to the maximum of the brightness distribution obtained by convolving the delta components of the CLEAN model with the corresponding synthesized beam (but see below). To remove the effects of the ionosphere on our phase delays as accurately as possible, we tried to ensure that the reference points selected in the maps at 8.4 and 2.3 GHz corresponded to the same point in the sky, despite the frequency dependence of both opacity and resolution effects. For 1928+738 at 8.4 GHz, we have labelled the inner components (see Fig. 1) as X1, X2, and X3 (which may correspond to components A, A1, and C, respectively, in the coeval 22 GHz maps of Hummel et al. 1992). Component X1 is likely the core, and X2 and X3 travelling jet components; our reference point at 8.4 GHz is the apparent peak of X2, the brightest feature. At 2.3 GHz these three components are blended, and our reference point (S1) is likely weighted more by the jet components X2 and X3 than by component X1, since the last is associated with the core and likely to have a more inverted spectrum than either X2 or X3. Therefore, the peak of brightness at 2.3 GHz likely corresponds to some point between components X2 and X3 in the 8.4 GHz image. We adopted this registration and aligned the peak of brightness of the 2.3 GHz image with the midpoint between components X2 and X3, dropping thereby the initial assumption that the origins of the two maps correspond to the same point on the sky. We thus identified the origin of the 2.3 GHz map with a point in the 8.4 GHz map 0.5 mas away, along PA 165°. We assigned an uncertainty of 0.5 mas to this registration to cover all positions between the 8.4 GHz components X2 and X3. For 2007+777 at 8.4 GHz, the peak of brightness seems to coincide with the easternmost component, probably the core (Fig. 2). At 2.3 GHz, with a coarser resolution and a smaller contrast between the core and jet components (due to the different spectral indices of the two components), the location of the peak of brightness is a weighted average of the positions of the core and the jet component. We thus registered the peak of brightness of the 2.3 GHz image with the midpoint between the core and jet components of the 8.4 GHz image, that is, 0.6 mas along PA 260°. We assigned an uncertainty of 0.5 mas to the value above to cover all positions between the 8.4 GHz core and the jet component.

3.2. Propagation-medium corrections

We modelled the tropospheric zenith delay at each station as a piecewise-linear function characterized by values specified at epochs four hours apart. A priori values at these nodes were calculated from local surface temperature, pressure, and humidity, based on the model of Saastamoinen (1973). The use of more nodes produced insignificant changes in the final results. We used the dry and wet Chao mapping functions to determine the tropospheric delay at non-zenith elevations, i.e., along the line of sight for each observation at each site. Since the antenna elevations were always higher than 20°, more elaborate mapping functions would have yielded similar astrometric results.

For each site, we combined our simultaneous, virtually source-structure-free, connected phase delays at 8.4 and 2.3 GHz to remove the plasma contribution (mainly due to Earth's ionosphere), taking advantage of its ν^{-2} dependence. The absence of 2.3 GHz data from Bonn forced us to follow a different procedure to remove the ionospheric contribution from the observables of the baselines involving this station. An estimate of the ionospheric delay –with the proper sign– can in principle be made from the 8.4 GHz data alone by calculating half

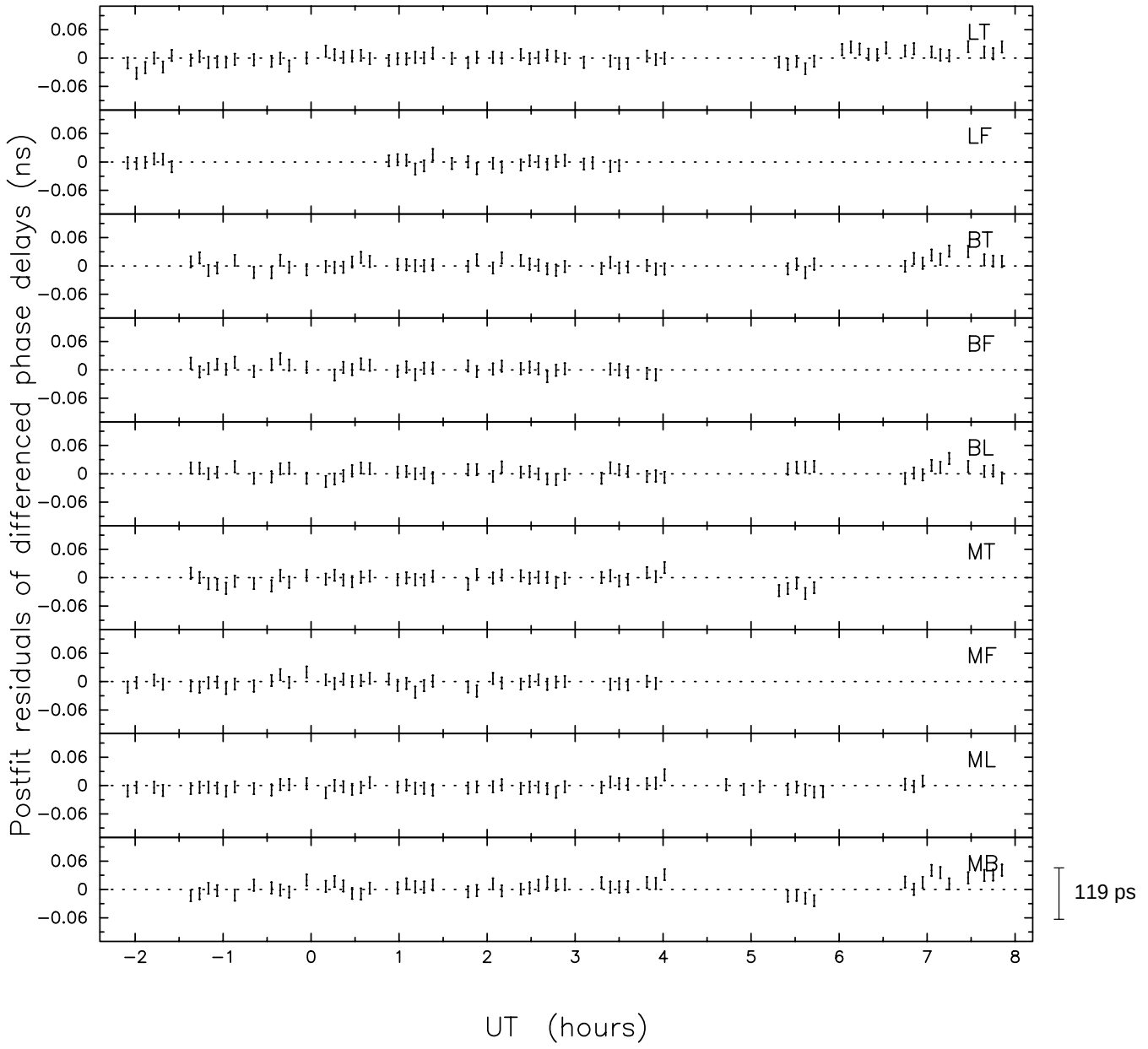

Fig. 3. Postfit residuals of the "plasma-freed" differenced phase-delays for 1988.83. These delays were constructed by subtracting each phase delay for 2007+777 from the previous one for 1928+738. Each error bar shown extends minus to plus one standard deviation of the corresponding differenced phase delays. Those errors were set to a constant value such that the χ^2 per degree of freedom of the postfit residuals was unity. The size of one 8.4 GHz ambiguity interval (119 ps) is also shown. The antenna codes are those given in Table 1.

the difference between each group delay and its corresponding (connected) phase delay; however, even for the most sensitive baseline, MB, the rms scatter of these estimates was $\sim$0.2 ns, which is larger than a phase-delay ambiguity interval and, therefore, the use of such ionospheric estimates in our phase-delay analysis would have degraded the quality of our astrometric determinations. Instead, for each observation for the MB baseline, we estimated the ionospheric delay by shifting in time the dual-frequency ionospheric estimates for the baselines MT and ML to account for the differences in longitude between Onsala and Medicina on the one hand and Bonn on the other, and then averaging the shifted values for MT and ML. (Note that the latitude of Bonn, 50° N, is about halfway between that of Medicina, 44° N, and Onsala, 57° N.) We are assuming that the ionosphere varies linearly across Europe. This assumption has proved to be successful for differential astrometry at other epochs (e.g., G95). In our case, further support for the smoothness of the ionosphere over the stations involved is provided by the similarity between the ionospheric contribution for the baselines ML and MT: the largest difference between the ionospheric delays for these two baselines is $\sim$0.1 ns, nearly an order of magnitude smaller than the maximum difference delay for each of these baselines. The

Table 2. Estimates of the coordinates (J2000) of 1928+738 minus those of 2007+777[1].

Epoch	Frequency	$\Delta\alpha + 37^m\,42^s.50333$		$\Delta\delta + 3^\circ\,54'\,41''.6778$
	(GHz)	(ms)	(mas)	(mas)
1985.77	5	-0.002 ± 0.070	-0.01 ± 0.25	-0.16 ± 0.15
1988.83	8.4 & 2.3	-0.036 ± 0.055	-0.13 ± 0.20	0.57 ± 0.13

[1] The reference relative position is that of the 1994 IERS Annual Report.
To express the values of $\Delta\alpha$ in milliarcseconds, we have added a column in which we multiplied $\Delta\alpha$ by the factor $15\cdot\cos\delta_m$, where δ_m is the mean declination of 1928+738 and 2007+777 ($\sim 76^\circ$). The uncertainties shown are statistical standard errors scaled so that the χ^2 per degree of freedom of the postfit residuals for the difference observables is unity.

Table 3. Contributions to the standard errors of the estimates of the coordinates of 1928+738 minus those of 2007+777 ($\delta\Delta\alpha$, $\delta\Delta\delta$) from the sensitivity study.

Effect	1985.77 (5 GHz)[1]			1988.83 (8.4 & 2.3 GHz)		
	$\delta\Delta\alpha$[2]		$\delta\Delta\delta$	$\delta\Delta\alpha$		$\delta\Delta\delta$
	(ms)	(mas)	(mas)	(ms)	(mas)	(mas)
Ref. point identification	0.010	0.04	0.03	0.005	0.02	0.03
Earth's nutation	0.002	0.01	0.01	0.002	0.01	0.01
Plasma[3]	0.025	0.09	0.07	0.011	0.04	0.04
Statistical standard errors	0.070	0.25	0.15	0.055	0.20	0.13
Root-sum-square of the above contributions	0.08	0.27	0.17	0.06	0.21	0.14

[1] The error budget of the 5 GHz data from G95 is also included in this table to facilitate comparison with the dual frequency data.
[2] To express the values of $\Delta\alpha$ in milliarcseconds, we have added a column in which we multiplied $\Delta\alpha$ by the factor $15\cdot\cos\delta_m$, where δ_m is the mean declination of 1928+738 and 2007+777 ($\sim 76^\circ$).
[3] For the 5 GHz data these values reflect the standard deviations of the parameter values (period and phase) for the rectified cosine model used for simulating the total electron content evolution (see G95); for the dual-frequency data, these values reflect the assumed standard deviation in the 8.4/2.3 GHz map registration (see Guirado et al. 1995b).

ionospheric estimates for the other baselines involving Bonn were calculated by taking advantage of the closure of the ionospheric contribution to the phase delays, which must be zero for each triangle of stations. For example, the ionospheric delay for BF is just the difference between the contributions for the baselines MF, calculated by combining our dual frequency observations, and MB, calculated by shifting and averaging the dual-frequency estimates of MT and ML.

As stated above, after making the ionospheric correction, we again used weighted-least-squares to estimate, for each station, the overall number of ambiguities for our (nearly) structure-free, plasma-corrected phase delays; they turned out to be no more than about 0.1 (at 8.4 GHz) and so we fixed them to zero.

3.3. Relative position

We obtained our estimate of the relative position of the reference points in the two sources by weighted-least-squares analysis of the differenced phase delays, formed by subtracting the plasma-corrected phase delay of each observation of 2007+777 from the corresponding phase delay of the previous observation of 1928+738. These differenced delays are nearly free from errors due to inaccuracies in our models for the atmosphere, site coordinates, and Earth orientation. We also included the phase delays for 1928+738 in the analysis to estimate the relative behaviour of the station clocks (see G95). The postfit residuals of the differenced phase delays are shown in Fig. 3. The result for the coordinates of component X1 (see Fig. 1) of 1928+738 relative to the core of 2007+777 is shown in Table 2. The coordinates of the peak of brightness (associated with component C2; see below) of 1928+738 relative to the core of 2007+777 for the epoch 1985.77 at 5 GHz are also shown. To make a consistent comparison between these two positions, the 5 GHz data were re-analyzed in the same system as was used in the analysis of the 8.4/2.3 GHz data (i.e., a priori values of the antenna coordinates, source coordinates, and Earth-orientation parameters were taken from IERS 1994).

3.4. Error analysis

From an error analysis similar to the one described in G95 we determined the contribution to the standard error of our relative position from the a priori uncertainty of quantities not estimated in the weighted-least-squares analysis, namely, core location, nutation, and ionospheric plasma delays. To determine the standard deviation associated with the core identification and with Earth nutation we followed an identical procedure to that described in G95 (see Table 3). The standard deviation associated with the ionosphere is mainly due to errors in the registration of the maps at 8.4 and 2.3 GHz. We estimated in Sect. 3.1 that the errors in the registration of the maps at the two frequency bands were 0.5 mas for each source; the contribution of this error to the final result is scaled down by the factor $(R-1)^{-1}$ ($\sim$0.079, where R is the square of the ratio between the reference frequencies of the two bands; see Guirado et al. 1995b for details). The corresponding contributions are shown in Table 3. We note that, if the ionospheric contribution in 1988.83 were comparable to that in 1985.77, we would have expected the ionospheric

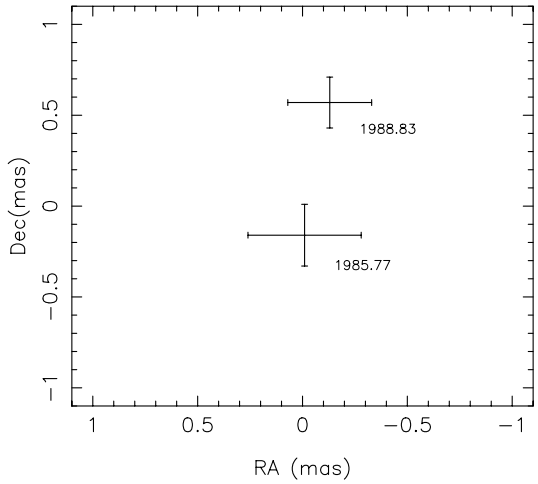

Fig. 4. Relative positions of 1928+738 with respect to 2007+777. The positions from Table 2 and their overall standard deviations from Table 3 are represented. The origin corresponds to the relative position obtained from IERS 1994.

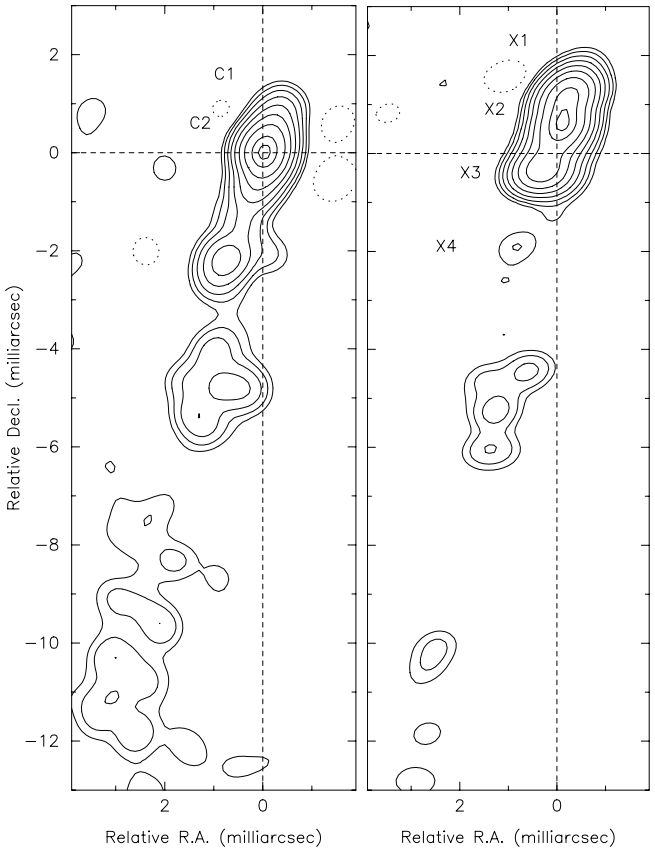

Fig. 5. Registration of the maps of 1928+738 at 5 GHz (epoch 1985.77; left image) and 8.4 GHz (epoch 1988.83; right image). The 5 GHz image has been overresolved by a factor of two to facilitate comparison with the 8.4 GHz map. For this registration the change in separation between the two sources (see Fig. 4) has been entirely attributed to changes in the structure of 1928+738.

contribution to the standard error to be ∼0.03 (by frequency scaling the 0.07 value at 5 GHz to 8.4 GHz). In any case, the error contribution for the ionosphere turned out to be less than one third of the statistical standard error. The overall standard deviation of each component of the estimated relative position of 1928+738 and 2007+777 was taken to be the root-sum-square of the standard deviations shown in Table 3.

4. Result and discussion

The relative positions of the radio sources 1928+738 and 2007+777 at the two epochs are represented in Fig. 4 with their standard deviations. This figure shows a significant net change with time of the relative declination of the selected fiducial points of the sources, while the right ascension change is not significantly different from zero. There are several phenomena that could, individually or in combination, explain such a change in separation: *1)* opacity effects on the apparent location of the fiducial point, *2)* a shift with respect to the center of mass of a selected fiducial point, due to the blending of the core with an emerging component, *3)* misidentification of the selected reference feature at different epochs, and *4)* motion of the center of activity (in particular, binary black-hole models of 1928+738 predict a precession of the core with amplitude ∼0.1 mas and period of ∼3 yr (Hummel et al. 1992); however, such an amplitude would be difficult to detect reliably with our data due to the possible presence of optical-depth effects which could not be separably detected even when comparing positions obtained at our two different frequency bands). We discuss these possibilities below.

What is the correct "registration" of the maps from each of the two sources for the two epochs of observation? In particular, to which source or sources do we attribute the change in separation that we obtained from the astrometry? It seems likely that the change in declination is due to changes in the inner structure of 1928+738, since this source appears to have a southward-directed jet with moving components, and transverse motions in the eastward-directed jet of 2007+777 are less likely. We interpret the null result for the change in relative right ascension as the absence of apparent motion in the region of 2007+777 near its core (as opposed, e.g., to both sources exhibiting similar motions in the same direction). Hence, we assume that the entire relative shift is due to changes within 1928+738, while 2007+777 behaves as a stationary reference source to within the limits set by our standard errors. The adopted registration is shown in Fig. 5 and Fig. 6 for 1928+738 and 2007+777, respectively. The corresponding change in the relative position of the peaks of brightness in the three years between 1985.77 and 1988.83 can be expressed as the vector change in position of the reference point in 1928+738 with respect to that in 2007+777, i.e., a vector of magnitude 0.74±0.22 mas along PA –9°±25°.

Such an apparent motion of the reference point in 1928+738 can be explained in terms of changes in the source structure between the two epochs and/or of changes in opacity effects between the two frequency bands. It seems unlikely that this "motion" corresponds to that of a particular component; it would need to be moving *towards* the core, which would be difficult to explain within standard relativistic jet models. More likely is

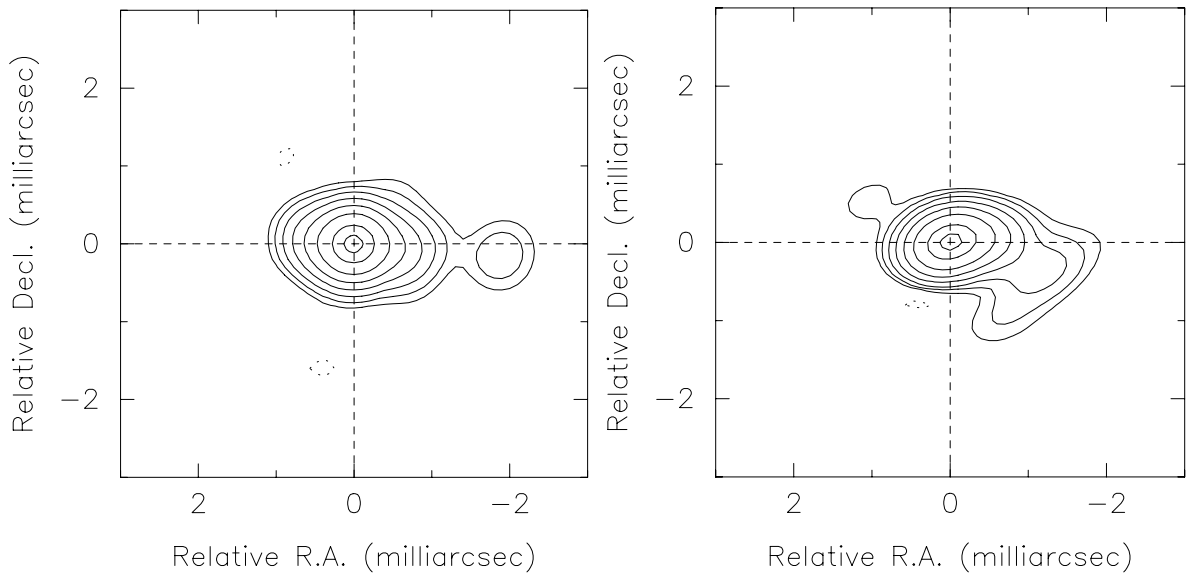

Fig. 6. Registration of the maps of 2007+777 at 5 GHz (epoch 1985.77; left image) and 8.4 GHz (epoch 1988.83; right image). As in Fig. 5, the 5 GHz map has been overresolved by a factor of two to facilitate comparison with the 8.4 GHz map

that the observed motion is a consequence of our failing to identify the same physical feature in 1928+738 as the reference point at the two epochs, i.e., that the peak of brightness corresponds to different jet components in each map. Supporting evidence for this hypothesis is the presence near 1988.83 of an emerging component in the maps of 1928+738 at 22 GHz (Hummel et al. 1992). This component could be associated with component X2, partially blended with the core in our 8.4 GHz map. The peak of the 5 GHz image (C2) in this scenario corresponds to a different jet component located further down the jet than component X2; it is unfortunately unclear whether the feature C1, elongated toward the north, is the core. According to this hypothesis, the shift detected in our astrometry should be part of a continuous motion of the peak of brightness. In this scenario, the peak of brightness moves as the brightest component travels down the jet (southwards for 1928+738); this motion would continue until the component fades and/or a new, and hence brighter, component is ejected; the peak of brightness would then be a blend of the new emerging component and the core, and a rapid shift of this peak towards the core (northwards for 1928+738) would occur. Such a rapid shift likely caused most or all of the difference in position we observed. For our maps, which were obtained at different radio frequencies for the two epochs, we would expect some contribution to the observed change in separation of the peak of brightness due to opacity effects that depend on frequency. However, given the relatively small difference between the frequencies of the maps (5 and 8.4 GHz), the observed change in separation between the sources ($\sim$0.7 mas) is probably too big to be produced solely by opacity effects (Marcaide & Shapiro 1984; Lara et al. 1996). Thus, although the observed change in separation is likely a combination of temporal and spectral changes of the source structure, the contribution of the former is probably considerably greater than that of the latter.

We can predict the position of component C2 in our 8.4 GHz map using the proper motion for the 5 GHz components of Schalinski (1990): 0.56$\pm$0.04 mas/yr; however, at the predicted position, the 8.4 GHz map shows just a trace of emission, labelled as X4 in Figs. 1 and 5, only 1% of the peak. This emission could correspond to C2, if C2 had faded rapidly as it traveled southwards.

5. Conclusion

We have used 5 GHz and 8.4/2.3 GHz VLBI observations of the radio sources 1928+738 and 2007+777 to deduce a change in the position of the peak of brightness of 1928+738 of 0.74$\pm$0.22 mas along PA –9°$\pm$25°between 1985.77 and 1988.83. This shift is attributed mostly to the presence of a new component emerging near epoch 1988.83, and, to an unknown, but lesser, degree, to frequency-dependent opacity effects. The measured change in separation could be part of a recurrent pattern of motion of the peak of brightness produced by components intermittently ejected from the core.

Our results indicate that at centimeter wavelengths the peak of brightness of 1928+738 does not correspond to its core, but to moving components. Therefore, even by comparing maps at similar frequency bands, it would be difficult to set a useful upper bound to the stability of the core, as the uncertainties would be dominated by those in the identification of the core in the maps. As for other sources, e.g., 4C 39.25 (Guirado et al. 1995b) and 1038+528 (Marcaide et al. 1994; Rioja et al. 1997), the limiting factor in the determination of relative position and proper motion is the uncertainty in the consistent identification of a reference point in the radio source maps from different epochs. Observations at higher resolution (i.e., millimeter VLBI and/or space VLBI) should alleviate this problem, since they of-

fer the possibility of matching the resolution of the radio source maps with the precision of the astrometry; in such observations, the selection of the reference point should be more straightforward and less uncertain. In addition, observations at two or more higher frequencies should allow the detection of inverted spectral features, associated with the core.

Acknowledgements. We wish to thank the staffs of all the observatories for their contribution to the observations, and to the MPIfR staff for their efforts during the correlation. We thank Dr. R. Schwartz for kindly providing MPIfR VLBI tapes. We also thank Drs. F. Mantovani and A. Alberdi for valuable comments on the manuscript. E.R. acknowledges a fellowship of the Generalitat Valenciana. This work has been partially supported by the Spanish DGICYT grant PB93-0030 and the U.S. National Science Foundation Grant AST89-02087.

References

Bartel N., Herring T.A., Ratner M.I., Shapiro I.I., Corey B.E., 1986, Nat, 319, 733
Eckart A., Witzel A., Biermann P., et al., 1986, A&A, 168, 17
Eckart A., Witzel A., Biermann P., et al., 1988, A&A Suppl. Ser., 67, 121
Guirado J.C., Marcaide J.M., Elósegui P., et al., 1995a [G95], A&A, 293, 613
Guirado J.C., Marcaide J.M., Alberdi A., et al., 1995b, AJ, 110, 2586
Hummel C.A., Schalinski C.J., Krichbaum T.P., et al., 1992, A&A, 257, 489
International Earth Rotation Service (IERS), Annual Report for 1993, 1994, Feissel M., and Essaïfi N. (eds.), (Paris)
Johnston K.J., Fey A.L., Zacharias N., et al., 1995, AJ, 110, 880
Lara L., Marcaide J.M., Alberdi A., Guirado J.C. 1996, A&A, 314, 672
Marcaide J.M., Shapiro I.I., 1984, ApJ, 276, 56
Marcaide J.M., Elósegui P., Shapiro I.I., 1994, AJ, 108, 368
Rioja M.J., Marcaide J.M., Elósegui P., Shapiro I.I., 1997, A&A, 325, 383
Robertson D.S., 1975, Ph.D. Thesis, Massachusetts Institute of Technology
Rogers A.E.E., Cappallo R.J., Hinteregger H.F., et al., 1983, Science, 219, 51
Saastamoinen J., 1973, Bull. Géodésique, 105, 279
Schalinski C.J., 1990, Ph.D. Thesis, Rheinische Friedrich-Wilhems-Universität zu Bonn
Shepherd M.C., Pearson T.J., Taylor G.B., 1995, BAAS, 26, 987
Witzel A., Schalinski C.J., Johnston K.J., et al., 1988, A&A, 206, 245